Spectroscopic Properties and Ligand Field Analysis of *cis*-Dinitrato(1,4,8,11-tetraazacyclotetradecane)chromium(III) Nitrate

Jong-Ha Choi

Department of Chemistry, Andong National University, Andong 760-749, Korea
Received January 16, 1997

The luminescence and photoexcitation spectra of *cis*-[Cr(cyclam)(NO$_3$)$_2$]NO$_3$·½H$_2$O (cyclam=1,4,8,11-tetraazacyclotetradecane) taken at 77 K are reported. The infrared and visible spectra at room-temperature are also measured. The vibrational intervals of the electronic ground state are extracted from the far-infrared and emission spectra. The ten electronic bands due to spin-allowed and spin-forbidden transitions are assigned. With observed transitions, a ligand field analysis has been performed to determine the bonding property of nitrate group in the chromium(III) complex. According to the results, it is found that nitrate ligand has weak σ- and π-donor properties toward chromium(III).

Introduction

The application of electronic spectroscopy to chromium (III) complexes promises to provide informations concerning metal-ligand bonding properties as well as molecular geometry.[1-8] The splittings of sharp-line electronic transitions are very sensitive to the bond angles around the metal. Thus it is possible to extract structural information from sharp-line electronic spectroscopy without a full X-ray structure determination.[9-11]

When nitrate ion forms complexes with transition metal ions, it can act as a unidentate, chelating bidentate, or bridging bidentate ligand types.[12] It is not easy to differentiate these nitrato coordinations because the symmetry of the nitrate ion little differs among them. However, infrared spectroscopy and normal coordinate analysis are helpful in determining the type of coordination.[13,14] A few of works have been done on the preparation and characterization of chromium(III) complex with the nitrato group.[15-17] The nitrato cyclam chromium(III) complex serves as the starting material for the preparation of all the other *cis* diacido species. Synthetic method and infrared spectral data of the title complex were reported.[18] However, so far literature give no information on the ligand field properties of coordinated nitrate group toward chromium(III).

In this study the 77 K luminescence and excitation spectra, and the room temperature infrared and visible spectra of *cis*-[Cr(cyclam)(NO$_3$)$_2$]NO$_3$·½H$_2$O were measured. The pure electronic origins were assigned by analyzing the absorption and excitation spectra. Using the observed electronic transitions, a ligand field analysis has been performed to determine the metal-ligand bonding properties for the coordinated atoms toward chromium(III).

Experimental

The free ligand cyclam was purchased from Strem Chemicals. All chemicals were reagent grade materials and used without further purification. The *cis*-[Cr(cyclam)(NO$_3$)$_2$]NO$_3$·½H$_2$O was prepared as described in the literature.[18] Found: C, 26.25; H, 5.33; N, 21.74. $C_{10}H_{25}N_7O_{9.5}Cr$ requires C, 26.85; H, 5.27; N, 21.83%. The microanalysis data are consistent with formation given and published values.[18] Analysis for C, H, and N was performed by Elemental Vario EL analyzer at Taegu division of KBSI.

The room-temperature visible absorption spectrum was recorded with a Hewlett-Packard 8452A diode array spectrophotometer. The mid-infrared spectrum was obtained with a Bruker IFS120HR/FRA106 FT-IR spectrometer on a KBr disk. The far-infrared spectrum in the region 600-50 cm^{-1} was recorded with a Bruker 113V spectrometer on a microcrystalline sample pressed into a polyethylene pellet. The emission and excitation spectra were measured at 77 K on a Spex Fluorolog-2 spectrofluorometer as described previously.[2]

All optimizations and calculations for the ligand field parameterization were performed on an IBM mainframe computer.

Results and Discussion

Absorption Spectrum. The visible absorption spectrum (solid line) of *cis*-[Cr(cyclam)(NO$_3$)$_2$]$^+$ in aqueous solution at room temperature is represented in Figure 1.

It exhibits two bands, one at 20533 cm^{-1} (ν_1) and the oth-

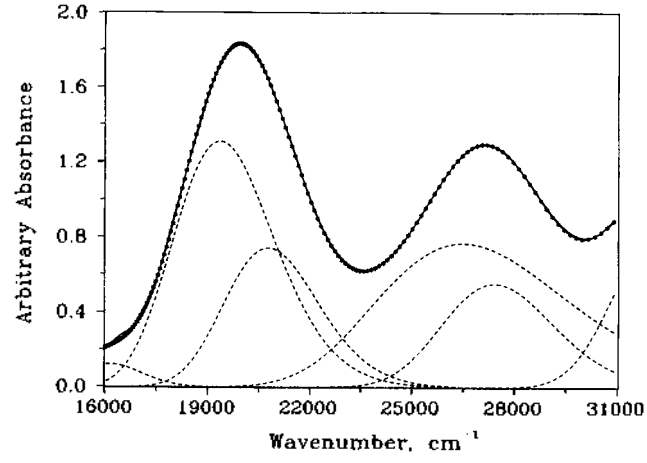

Figure 1. Resolved electronic absorption spectrum of *cis*-[Cr(cyclam)(NO$_3$)$_2$]$^+$ in aqueous solution at 298 K.

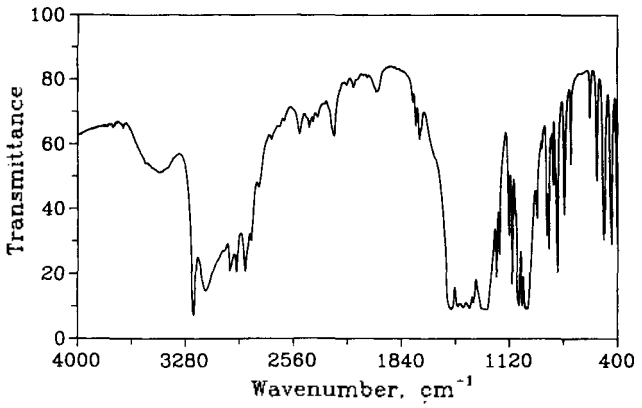

Figure 2. Mid-infrared spectrum of *cis*-[Cr(cyclam)$(NO_3)_2$]NO_3·½H_2O at 298 K.

er at 26955 cm^{-1} (ν_2), corresponding to the $^4A_{2g}\rightarrow{}^4T_{2g}$ and $^4A_{2g}\rightarrow{}^4T_{1g}$ (O_h) transitions, respectively.[19] The quartet bands have nearly symmetric profiles. In order to obtain some points of reference for the splittings of the two bands, the band profiles were fitted by using four Gaussian curves, as seen in Figure 1. The contribution from outside bands was corrected for the fine deconvolution. A deconvolution procedure on the experimental band pattern yielded maxima at 19805, 20780, 26400 and 27200 cm^{-1} for the noncubic splitttings of $^4T_{2g}$ and $^4T_{1g}$. These peak positions were used as the observed spin-allowed transition energies in the ligand field optimization.

Infrared Spectra. The mid- and far-infrared spectra of *cis*-[Cr(cyclam)$(NO_3)_2$]NO_3·½H_2O recorded at room temperature are presented in Figures 2 and 3.

The broad absorption near 3460 cm^{-1} can readily be assigned to the O-H stretching mode of the H_2O molecule in the hydrated complex. The two sharp peaks at 3225 and 3145 cm^{-1}, and the peaks in the 3000-2800 cm^{-1} region are due to the symmetric and asymmetric N-H and C-H stretching modes, respectively. The complex *cis*-Cr(cyclam)$(NO_3)_3$·½H_2O could be formulated as *cis*-[Cr(cyclam)$(NO_3)_2$]NO_3·½H_2O with unidentate nitrate or as *cis*-[Cr(cyclam)NO_3]$(NO_3)_2$·½H_2O containing bidentate nitrate. General nitrate complexes exhibit intense absorption bands in the region 1000-1020, 1270-1280 and 1510-1520 cm^{-1} due to unidentate nitrate[16] while free nitrate absorptions appear at 710-730, 820-830, 1050-1060 and 1380-1390 cm^{-1}.[12] The four absorptions at 709, 827, 1056 and 1386 cm^{-1} are assigned to the ν_4, ν_2, ν_1, and ν_3 modes of ionic nitrate, respectively. The far-infrared spectrum of the title complex is remarkably similar to that of *cis*-[Cr(cyclam)$(NO_3)(H_2O)$]NO_3 although it contains *cis*-[Cr(cyclam)$(NO_3)_2$]NO_3·H_2O as an impurity. The existence of impurity in *cis*-[Cr(cyclam)$(NO_3)(H_2O)$]NO_3 was confirmed by measuring emission and excitation spectra at 77 K. The spectrum of *cis*-[Cr(tet *b*)$(NO_3)_2$]NO_3 has infrared bands at 1515, 1290, and 1000 cm^{-1}.[17] The tet *b* complex has limited solubility in DMSO giving Λ_M=85 ohm^{-1}cm^{2}mol^{-1} at 25 °C consistent with a 1:1 electrolyte and two unidentate nitrate ligands.[17] I believe that the coordinated structures of nitrate in both complexes are the same. The title complex has strong infrared absorptions at 1511, 1288 and 1005 cm^{-1}. The above data support the unidentate nature of the nitrato group. It is also substantiated by the small splitting of bands appearing at 1763 and 1743 cm^{-1}.[13] The strong peaks at 445 and 491 cm^{-1} can be assigned to the Cr-N stretching mode.[9] A number of absorption bands below 402 cm^{-1} arise from lattice vibration, skeletal bending and the Cr-ONO_2 stretching mode.

Luminescence Spectrum. An experimental problem lies with the difficulty in distinguishing pure electronic components from the vibronic bands that also appear in the excitation spectrum. The vibrational intervals due to the electronic ground state can be obtained by comparing the emission spectrum with far-infrared spectral data. The 490 nm excited 77 K luminescence spectrum of *cis*-[Cr(cyclam)$(NO_3)_2$]NO_3·½H_2O is shown in Figure 4. The band positions relative to the lowest zero phonon line, R_1, with corresponding infrared frequencies, are listed in Table 1. The luminescence spectrum was independent of the exciting wavelength within the first spin-allowed transition region.

The strongest peak at 14440 cm^{-1} is assigned as the zero-phonon line, R_1, because a corresponding strong peak is found at 14444 cm^{-1} in the excitation spectrum. A well defined hot band at 14501 cm^{-1} may be assigned to the second component of the $^2E_g\rightarrow{}^4A_{2g}$ transition. The vibronic intervals occurring in the spectrum consist of several modes

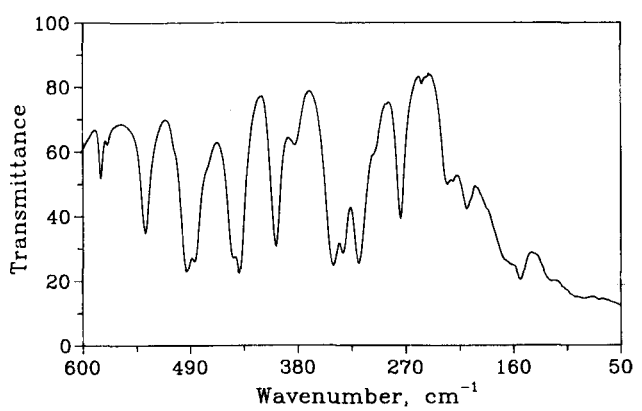

Figure 3. Far-infrared spectrum of *cis*-[Cr(cyclam)$(NO_3)_2$]NO_3·½H_2O at 298 K.

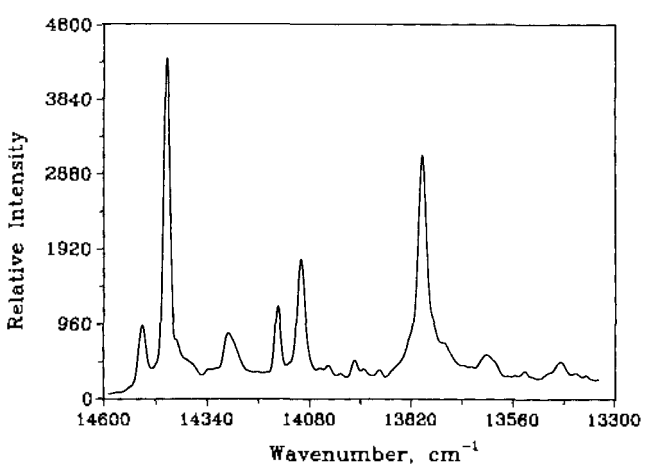

Figure 4. The 77 K luminescence spectrum of *cis*-[Cr(cyclam)$(NO_3)_2$]NO_3·½H_2O (λ_{ex}=490 nm).

Table 1. Vibrational Frequencies from the 77 K Lminescence and 298 K Infrared Spectrum for *cis*-[Cr(cyclam)(NO$_3$)$_2$]NO$_3$· ½ H$_2$O[a]

Luminescence[b]	Infrared	Assignment
-61 s		R_1
0 vs		R_2
106 w, 125 w	122 sh	Lattice vib., Skeletal bends, and ν(Cr-ONO$_2$)
155 m, 170 sh	154 m, 171 sh	
208 m, 230 vw	206 vw, 228 vw	
281 s	276 s	
339 vs	319 s, 335 m, 344 s	
388 vw	384 m	
409 w	402 s	
440 w	444 vs	ν(Cr-N)
478 m, 500 w	491 vs	
540 w	536 s	ν(Cr-N) + Ring def.
594 sh	582 m	
650 vs		
707 sh	709 m	NO$_3$ ion
757 vw	752 s	
776 vw	801 vs	
813 m	812 w	ρ(CH$_2$)
837 sh	827 m	NO$_3^-$ ion
869 vw	858 s, 870 s	ρ(NH$_2$)
911 w	935 m	
1002 m	997 s, 1015 s	
1042 w	1037 s	
1068 w	1056 vs	NO$_3$ ion

[a] Data in cm^{-1}. [b] Measured from zero-phonon line at 14440 cm^{-1}.

that can be presumed to involve primarily ring torsion and angle-bending modes with frequencies in the range 133-379 cm^{-1}. The bands at 440 and 478 cm^{-1} can be assigned to a Cr-N stretching mode.

Excitation Spectrum. The 77 K excitation spectrum is shown in Figure 5. It was recorded by monitoring a relatively strong vibronic peak in the luminescence spectrum. The spectrum obtained was independent of the vibronic peak used to monitor it. The peak positions and their assignments are tabulated in Table 2. The calculated frequencies in parentheses were obtained by using the vibrational modes ν_1-ν_4 listed in Table 2.

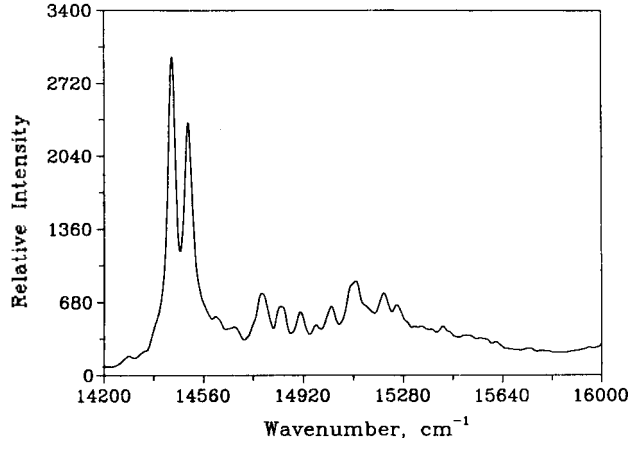

Figure 5. The 77 K excitation spectrum of *cis*-[Cr(cyclam)(NO$_3$)$_2$]NO$_3$· ½ H$_2$O (λ_{em}=725 nm).

Two strong peaks at 14444 and 14504 cm^{-1} in the excitation spectrum are assigned to the two components (R_1 and R_2) of the $^4A_{2g}\rightarrow{}^2E_g$ transition. The lowest-energy zero-phonon line coincides with the luminescence origin within 4 cm^{-1}. The zero-phonon line in the excitation spectrum splits into two components by 60 cm^{-1}, and it can be compared with those of the chromium(III) complexes with tetragonal symmetry.[20] In general, it is not easy to locate positions of the other electronic components because the vibronic sidebands of the ^2E_g levels overlap with the zero phonon lines of $^2T_{1g}$. However, the three components of the $^4A_{2g}\rightarrow{}^2T_{1g}$ electronic origin (T_1, T_2 and T_3) are assigned to relative intense peaks at 574, 664 and 765 cm^{-1} from the lowest electronic line, R_1. Vibronic satellites based on these origins also have similar frequencies and intensity patterns to those of the ^2E_g components.

The higher energy $^4A_{2g}\rightarrow{}^2T_{2g}$ band was found at 21980 cm^{-1} from the second derivative of the solution absorption spectrum, but it could not be resolved into the separate components.

Ligand Field Analysis. The ligand field potential matrix was generated for *cis*-[Cr(cyclam)(NO$_3$)$_2$]$^+$ from the coordinated four nitrogen and two oxygen atoms. No crystal

Table 2. Peak Positions in the 77 K Sharp-Line Excitation Spectrum of *cis*-[Cr(cyclam)(NO$_3$)$_2$]NO$_3$· ½ H$_2$O[a]

$\bar{\nu}_0$-14700	Assignment	(Calcd)[b]		Vibronic frequencies	Ground state frequencies[c]
0 vs	R_1		ν_1	175	171
60 vs	R_2		ν_2	274	276
159 w	$R_1+\nu_1$	(175)	ν_3	330	335
227 w	$R_2+\nu_1$	(235)	ν_4	467	478
327 s	$R_1+\nu_3$	(330)			
397 m	$R_2+\nu_3$	(390)			
466 m	$R_1+\nu_4$	(467)			
522 w	$R_2+\nu_4$	(527)			
574 m	T_1				
648 sh	$R_1+\nu_1+\nu_4$	(642)			
664 vs	T_2				
708 sh	$R_2+\nu_1+\nu_4$	(702)			
765 s	T_3				
812 m	R_1+812				
849 sh	$T_1+\nu_2$	(848)			
875 vw	R_2+815				
900 w	$T_1+\nu_3$	(904)			
936 vw	$T_3+\nu_1$	(940)			
979 m	T_1+405				
1007 w	T_1+433				
1062 vw	T_1+488				
1113 w	$T_3+2\nu_1$	(1115)			
1135 vw	$T_2+\nu_4$	(1131)			
1171 w	T_3+406				
1336 vw	T_2+672				
1361 w	T_3+596				
1513 vw	$T_3+\nu_2+\nu_4$	(1506)			

[a] Data in cm^{-1}. [b] Values in parentheses represent the calculated frequencies based on the vibrational modes listed. [c] From the luminescence spectrum (Table 1).

structure for a salt of the complex ion is known, thus the positional parameters were adapted from the molecular geometry based on a molecular mechanics calculation.[2] The coordinates were then rotated so as to maximize the projections of the six-coordinated atoms on the Cartesian axes centered on the chromium. The resulting Cartesian and spherical coordinates are shown in Table 3.

Angular overlap model (AOM) parameters provide more chemical insight than crystal field parameters, and will be used to interpret the electronic spectra.[19] The π-interaction of the nitrato oxygen with the metal ion was considered to be anisotropic. The anisotropy of metal-ligand π-interaction can be expressed by e_π parameters in two perpendicular directions, denoted $e_{\pi s}$ and $e_{\pi c}$. By rotation of coordinates through the angle ψ, the value of $e_{\pi c}$ can be set to zero, and the π-interaction of the ligand expressed entirely through $e_{\pi s}$. The ligand field analysis was carried out through an optimized fit of experimental to calculated transition energies. Diagonalization of the 120×120 secular matrix yields the doublet and quartet energies with the appropriate degeneracies.[21] Hoggard has described the methods for determining the eigenvalues and eigenfunctions of a d^3 ion in a ligand field from any number of coordinated atoms.[11] The full set of 120 single-term antisymmetrized product wavefunctions was employed as a basis. The Hamiltonian used in the calculation was

$$\hat{H} = \sum_{i<j} \frac{e^2}{r_{ij}} + V_{LF} + \zeta \sum_i \boldsymbol{l}_i \cdot \boldsymbol{s}_i + \alpha_T \sum_i \boldsymbol{l}_i^2 + 2\alpha_T \sum_{i<j} \boldsymbol{l}_i \cdot \boldsymbol{l}_j \qquad (1)$$

where the terms in the right-hand side represent the interelectronic repulsion, ligand field potential, and spin-orbit coupling, respectively, with the last two representing the Trees correction.[22] The parameters varied during the optimization were the interelectronic repulsion parameters *B*, *C* and the Trees correction parameter α_T, the spin-orbit coupling parameter ζ, the AOM parameters $e_\sigma(NO_3)$ and e_π (NO_3) for the nitrate oxygen-chromium, and $e_\sigma(N)$ for the cyclam nitrogen-chromium. The π-interaction of amine nitrogens with sp^3 hybridization in the cyclam was assumed to be negligible. However, it is noteworthy that the peptide nitrogen with sp^2 hybridization has a weak π-donor character.[2] Schmidtke's π-expansion parameter τ were also included in the treatment of the interelectronic repulsion term. In Schmidtke's approximation, the electrostatic terms are modified by a factor τ for each constituent metal wavefunction that overlaps with a ligand π-orbital. The π-orbital expansion parameter, τ was fixed at the value 0.999. The estimated value was based on the analysis of $[Cr(NH_3)_5Cl]Cl_2$.[23] The Racah parameter, *A* was also fixed at 10000 cm^{-1}. The value of the Racah parameter, *A* has little effect on the calculated transition energies. All parameters, except e_σ (NO_3) and e_π (NO_3), were constrained to reasonable limits based on the data from other chromium(III) complexes. The seven parameters were used to fit eleven experimental energies: the five $^4A_{2g} \rightarrow \{^2E_g, {}^2T_{1g}\}$ components, identified in Table 4, the average energy of the transition to the $^2T_{2g}$ state, the four $^4A_{2g} \rightarrow \{^4T_{2g}, {}^4T_{1g}\}$ components, and the splitting of the ^2E_g state. Eigenvalues were assigned to states within the doublet and quartet manifolds based on an analysis of the corresponding eigenfunctions. The function minimized was

$$f = 10^3 S^2 + 10^2 \sum D^2 + 10\, T^2 + \sum Q^2 \qquad (2)$$

where *S* in the first term is the ^2E_g splitting, and *D*, *T*, and *Q* represent the differences between experimental and calculated $\{^2E_g, {}^2T_{1g}\}$, $^2T_{2g}$, and $\{^4T_{2g}, {}^4T_{1g}\}$ transition energies, respectively. The Powell parallel subspace optimization procedure[24] was used to find the global minimum. The optimization was repeated several times with different sets of starting parameters to verify that the same global minimum was found. The results of the optimization and the parameter set used to generate the best-fit energies are also listed in Table 4. The fit is very good for the sharp line transitions. The error margins reported for the best-fit parameters in Table 3 are based only on the propagation of the assumed uncertainties in the observed peak positions.[25] The quartet terms were given a very low weight to reflect the very large uncertainty in their position.

The following values were finally obtained for the ligand field parameters: $e_\sigma(N)$=7505±20, $e_\sigma(NO_3)$=5848±46, e_π (NO_3)=786±31, *B*=722±2, *C*=2774±11, α_T=132±4, and ζ=275±36 cm^{-1}. The position and splitting of sharp-line transitions are analyzed as a function of the $e_\pi(NO_3)$ parameter as shown in Figure 6. All other ligand field parameters are given at the bottom of Table 3. It is apparent that the splitting of the ^2E_g zero-phonon line increases with the π-donor property of the nitrate group.

The sharp-line splitting seems to be very sensitive to the

Table 3. Optimized Cartesian and Spherical Polar Coordinates for Ligating Atoms and Adjacent Nitrogens in *cis*-$[Cr(cyclam)(NO_3)_2]^+$[a]

Atom	*x*	*y*	*z*	θ	φ	ψ
O_1	−0.0067	−2.3257	0.0081	89.78	90.19	18.97
O_2	−0.0120	0.0188	−2.3326	179.42	123.29	−23.32
N_1	2.0823	−0.1310	−0.0345	90.97	−3.63	0.00
N_2	0.0617	2.0987	−0.0599	91.64	88.29	0.00
N_3	−2.0842	0.1995	−0.1282	93.53	−174.53	0.00
N_4	0.0802	−0.0479	2.1030	2.58	−31.06	0.00
$N_1(O_1)$	−0.1707	−2.7548	0.4833			
$N_2(O_2)$	−0.7885	0.5324	−2.6487			

[a] Cartesian coordinates in Å, polar coordinates in degrees.

Table 4. Experimental and Calculated Electronic Transition Energies for *cis*-$[Cr(cyclam)(NO_3)_2]NO_3 \cdot \frac{1}{2} H_2O$[a]

State(O_h)	Exptl	Calcd[b]
^2E_g	14444	14440
	14504	14500
$^2T_{1g}$	15018	15000
	15108	15150
	15209	15200
$^2T_{2g}$(avg)	21980	21530
$^4T_{2g}$	19805[c]	19600
	20780[c]	20635
$^4T_{1g}$	26400[c]	26383
	27200[c]	27305

[a] Data in cm^{-1}. [b] $e_\sigma(N)$=7505±20, $e_\sigma(NO_3)$=5848±45, $e_\pi(NO_3)$=786±30, *B*=722±5, *C*=2774±10, *T*=132±5, ζ=275 35. [c] Obtained from the Gaussian component deconvolution.

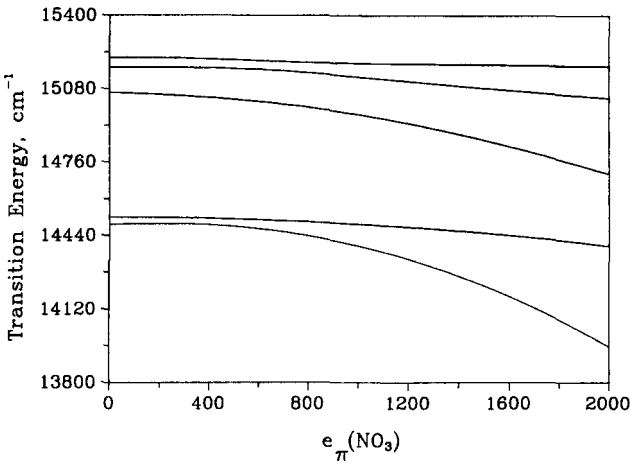

Figure 6. Calculated variation of the transition energies to the ^2E_g and $^2T_{1g}$ states for *cis*-[Cr(cyclam)(NO$_3$)$_2$]$^+$ as a function of e_π(NO$_3$).

extent of anisotropic π-bonding, and is well suited to decide the proper value of the e_π(NO$_3$) parameter. A ligand field analysis of the sharp-line excitation and broad-band absorption spectra indicates that the oxygen of nitrate is a weak σ-and π-donor. These values were lower than the values for other coordinated atoms in chromium(III) complexes.[1-11] It seems that the attached NO_2 group weakens the bonding ability of the coordinated oxygen in the nitrate ligand. The value of 7509 cm^{-1} for e_σ(N) is comparable to values for other amines.[8,9,26] It is suggested that the four nitrogen atoms of the macrocyclic ligand cyclam have strong σ-donor properties toward chromium(III). The AOM parameters can be used in interpreting the preferential photosolvation and photostereochemistry of transition metal complexes.[27] The observed ^2E_g splitting, 60 cm^{-1} in the excitation spectrum is small compared with the 139 cm^{-1} of *cis*-[Cr(cyclam)Cl$_2$]Cl.[4] An orbital population analysis yields a configuration of $(xy)^{0.976}(xz)^{1.002}(yz)^{0.991}(x^2\text{-}y^2)^{0.08}(z^2)^{0.02}$ for the lowest component of the ^2E_g state. The relative *d*-orbital ordering from the calculation is $E(xy)$=126 cm^{-1}<$E(xz)$=652 cm^{-1}<$E(yz)$=1225 cm^{-1}<$E(x^2\text{-}y^2)$=19984 cm^{-1}<$E(z^2)$=21295 cm^{-1}. The value of the Racah parameter *B* is about 70% of the value for a free chromium(III) ion in the gas phase. The parameter values reported here appear to be significant, as deduced on the basis of the manifold of sharp-line transitions which were obtained from the highly resolved excitation spectrum.

Acknowledgment. Financial support of the Korea Science & Engineering Foundation and the Deutsche Forschungsgemeinschaft are gratefully acknowledged. The author wishes to thank Prof. Patrick E. Hoggard for fruitful cooperation and Dr. Thomas Schönherr for measurements of far-infrared spectra.

References

1. Hoggard, P. E. *Top. Curr. Chem.* **1994**, *171*, 114.
2. Choi, J. H.; Hoggard, P. E. *Polyhedron* **1992**, *11*, 2399.
3. Choi, J. H. *Bull. Korean Chem. Soc.* **1993**, *14*, 118.
4. Choi, J. H. *J. Korean Chem. Soc.* **1995**, *39*, 501.
5. Choi, J. H. *J. Photosci.* **1996**, *3*, 43.
6. Choi, J. H.; Oh, I. G.; Yeh, J. H. *Korean Appl. Phys.* **1996**, *9*, 722.
7. Choi, J. H.; Oh, I. G. *Bull. Korean Chem. Soc.* **1997**, *18*, 23.
8. Choi, J. H.; Oh, I. G. *Bull. Korean Chem. Soc.* **1993**, *14*, 348.
9. Choi, J. H. *Bull. Korean Chem. Soc.* **1994**, *15*, 145.
10. Choi, J. H.; Lee, T. H. *Korean Appl. Phys.* **1994**, *7*, 186.
11. Hoggard, P. E. *Coord. Chem. Rev.* **1986**, *70*, 85.
12. Rosenthal, M. R. *J. Chem Edu.* **1973**, *50*, 331.
13. Lever, A. B. P.; Mantovani, E.; Ramaswamy, B. S. *Can. J. Chem.* **1971**, *49*, 1957.
14. Hester, R. E.; Grossman, W. E. L. *Inorg. Chem.* **1966**, *5*, 1308.
15. Chandra, S.; Sharma, K. K. *Synth. React. Inorg. Met. Org. Chem.* **1982**, *12*, 647.
16. Rai, P. K.; Gupta, A. K.; Prasad, R. N. *Bull. Korean Chem. Soc.* **1993**, *14*, 179.
17. House, D. A.; Hay, R. W.; Ali, M. A. *Inorg. Chim. Acta* **1983**, *72*, 239.
18. Kane-Maguire, N. A. P.; Wallace, K. C.; Miller, D. B. *Inorg. Chem.* **1985**, *24*, 597.
19. Lever, A. B. P. *Inorganic Electronic Spectroscopy*; Elsevier: Amsterdam, 1984.
20. Flint, C. D.; Matthews, A. P. *J. Chem. Soc., Faraday II.* **1973**, *69*, 419.
21. Smith, B. T.; Boyle, J. M.; Dongarra, J. J.; Garbow, B. S.; Ikebe, Y.; Klema, V. C.; Moler, C. B. *Matrix Eigensystem Routines-EISPACK Guide*; Spring-Verlag: Berlin, 1976.
22. Trees, R. E. *Phys. Rev.* **1951**, *83*, 756.
23. Schmidtke, H. H.; Adamsky, H.; Schönherr, T. *Bull. Chem. Soc. Jpn.* **1988**, *61*, 59.
24. Kuester, J. L.; Mize, J. H. *Optimization Techniques with Fortran*; McGraw-Hill: New York, 1973.
25. Clifford, A. A. *Multivariate Error Analysis*; Wiley-Hasted: New York, 1973.
26. Lee, K. W; Hoggard, P. E. *Transition Met. Chem.* **1991**, *16*, 377.
27. Vanquickenborne, L. G.; Ceulemans, A. *Coord. Chem. Rev.* **1983**, *48*, 157.